Synchronizing hyperchaotic volume preserving maps and circuits

Thomas L. Carroll and Louis M. Pecora

Abstract. We show that it is possible to synthesize chaotic systems that have improved characteristics for use in communications. These include whiter spectrum, low time correlation, hyperchaotic behavior, and little or no phase space structure. These systems are based on locally volume-preserving (or expanding) maps. We show how to construct a circuit that produces such characteristics.

I. Introduction

It has been established that chaotic circuits may be used to transmit information by synchronization or other means [1-7]. Most demonstrations of chaotic synchronization have taken place in dissipative systems, although chaotic synchronization in volume-preserving systems has also been demonstrated [8]. The attractors in dissipative systems have well defined structure or patterns and do not cover all of phase space. This is usually undesirable for spread spectrum communications and/or low-probability-of-intercept (LPI) signals. Furthermore, typical dissipative systems have spectra that still have identifiable peaks and/or "1/f" type fall-off. These lead to long time correlations. Signals for spread spectrum communications should have only short-time correlations and broad power spectra [9] . Usually, such signals are produced by pseudonoise generators. Synchronizing a pseudonoise generator in a receiver is complicated and may take a long time.

We show below that it is possible to produce a chaotic signal that has a flat spectrum and near delta-function autocorrelation while maintaining the short synchronization times typically seen for chaotic synchronization. We also demonstrate a communications circuit in which we transmit information by a chaotic carrier.

The chaotic circuit that we describe here is based on a locally volume-preserving hyperchaotic map. By locally volume preserving, we mean that the map is volume preserving within some defined region. Since volume-preserving systems do not have attractors, the chaotic motion may, for some systems, cover a large part or even all of the phase space. Chaotic motion that covers most of the phase space may result in a signal with a broad band power spectrum and an autocorrelation function that quickly drops to zero. Both of these characteristics are desirable for pseudonoise generators. Broad band signals improve resistance to interference in spread-spectrum systems, while generating many signals with low correlations increases the number of useful spreading codes [9]. Signals with quickly decreasing autocorrelations also are useful for linear system identification [10]. However, unlike most pseudonoise generators, chaotic systems may be self synchronizing, making it easy to detect changes in the chaotic signal.

In this work, we synchronize two hyperchaotic maps and send an information signal between them. The maps have no apparent attractors, so the resulting chaotic motion fills the phase space, resulting in a chaotic signal with a very broad power spectrum. We have also built these maps in circuit form, and we show here that the circuits may be synchronized. Building analog map circuits can be more complicated than building analog circuits to simulate flows, but if one plans to immediately digitize the circuit output, a map circuit naturally interfaces with a digital circuit, since both require an external clock. One could also build the entire system as a digital map circuit. The analog circuit has the potential for being faster and simpler with true non-periodic behavior for all times, but parameter matching is a problem in analog circuits that would not exist in a completely digital circuit. Finally, we describe variations on these maps that may be easier to construct as circuits. The variations we describe have some similarities to analog feedback shift registers described by Gershenfeld and Grinstein [11], although their systems were dissipative.

II. The Map

We can construct a locally volume preserving map by producing a system that is everywhere expanding in certain directions and contracting in other directions at the same rates so the volume is preserved. We couple the expanding and contracting parts of the map so no direction can shrink to zero. In order to keep the motion confined to a compact region of phase space we merely "fold" the trajectories back into that region whenever the expansion takes them beyond it. A simple way to do this is to have a linear map with the proper eigenvalues and unit determinant. We accomplish the fold either by a modulus shift, as in the Bernoulli map, or a "reflective fold" as in the tent map. We detail such systems below. Other variations are possible and we will cover these and broader synchronization issues elsewhere [12]. We use a very simple chaotic map:

$$\left.\begin{aligned} x_{n+1} &= -\left(\frac{4}{3}\right)x_n + z_n \\ y_{n+1} &= \left(\frac{1}{3}\right)y_n + z_n \\ z_{n+1} &= x_n + y_n \end{aligned}\right\}(\xi + 2)\bmod 4 - 2 \tag{1}$$

where "(ξ + 2)mod4 - 2" means that every iteration we take *x*, *y* or *z*, add 2, divide by 4, keep the remainder and subtract 2. Figure 1 is a graph of this modulus function. This map is quite similar to the cat map [13]

The Jacobian of the map in eq. (1) is linear, so the Lyapunov exponents (determined from the eigenvalues of the Jacobian) are 0.6829, 0.3023, and -0.9852. The exponents add to zero, so the map is locally volume preserving [13]. The presence of two positive Lyapunov exponents indicates hyperchaos.

It would seem that a map without dissipation could not be synchronized, but volume preserving maps must have contracting as well as expanding directions. Heagy and Carroll have shown how to synchronize volume preserving maps [8].

Our first choice for a subsystem for the map of eq. (1) is the *x*-*y* subsystem (we include *z*' in eq. (2) because it is simply a sum of *x*' and *y*'):

$$\begin{aligned} x'_{n+1} &= -\left(\frac{4}{3}\right)x'_n + z_n \\ y'_{n+1} &= \left(\frac{1}{3}\right)y'_n + z_n \\ z'_{n+1} &= x'_n + y'_n \end{aligned} \tag{2}$$

although one may see from the Jacobian for this subsystem that it is unstable. The modulus function is assumed in this and subsequent equations to save repetition. We may stabilize the subsystem of eq. (2) using the method of synchronous substitution [14]. We produce a new variable $w_n = z_n + \Gamma x_n$ from the drive system variables, and reconstruct a driving signal $\tilde{z}_n$ at the response system:

$$
\begin{aligned}
w_n &= z_n + \Gamma x_n \\
\tilde{z}_n &= w_n - \Gamma x'_n \\
x'_{n+1} &= -\left(\frac{4}{3}\right) x'_n + \tilde{z}_n \\
y'_{n+1} &= \left(\frac{1}{3}\right) y'_n + \tilde{z}_n \\
z'_{n+1} &= x'_n + y'_n
\end{aligned}
\tag{3}
$$

Synchronizing z'_n is trivial, since it is just a sum of the other two variables. Elsewhere we show that the synchronous substitution approach is similar to a recently applied control theory method [15]. The Jacobian for the x'-y' subsystem of the response system of eq. (3) is:

$$
\begin{bmatrix} -\frac{4}{3} - \Gamma & 0 \\ -\Gamma & \frac{1}{3} \end{bmatrix}
\tag{4}
$$

For $\Gamma = 0$, the response system is unstable, with eigenvalues of -4/3 and 1/3. If $\Gamma = -4/3$, the eigenvalues of the Jacobian are 1/3 and 0 and the subsystem is stable. Figure 2 shows z' synchronizing to z for the response map of eq. (3).

III. The Circuit

We built a circuit to simulate eqs. (1) and (3) to establish that these simple map systems were not so sensitive to noise or parameter mismatch would not prevent synchronization (to within a few per cent). Figure 3 is a block diagram of the circuit. The math unit used operational amplifiers as adders and subtractors to generate the math functions of eqs. (1) and (3). All resistors had 1% tolerance. The sample and hold circuits used a pair of alternately clocked LF398 sample and hold amplifiers to store values of the variables. The clock frequency for this circuit, generated by a 555 oscillator chip, was 6 KHz, although a range of clock frequencies is possible.

The modulus circuits performed the modulus function seen in Fig. 1. To limit the complexity of the circuit, the range of the circuit modulus function was limited to ±4 V. The modulus function uses two comparators to indicate when the input signal is greater than 2.0 V or less than -2.0 V. When these bounds are exceeded, an analog switch adds ± 4.0 V to the input signal so that the output signal remains within the range ±2.0 V. The block labeled "bounds" in Fig. 3 produced the reference signals for the modulus circuits.

Occasionally, one of the variables in the map circuit will exceed 4.0 V, resulting in an error in the modulus function. We have chosen the map of eq. (1) so that modulus errors did not happen too often. The modulus function, as all other parts of the circuit, was completely analog. The modulus function used uncompensated op amps (OP-37) so that the slew rate of the modulus function was much faster than the 6 KHz clocking rate of the circuit.

If the component variations were larger in the circuit (or noise was added to the transmitted signal), the largest effect on the response circuit was to cause mismatches in the modulus circuit to occur more often. The mismatches were seen as ± 4 volt spikes in the difference between input and output signals for the response circuit.

Figure 4 shows an output time series for the x_n variable from the circuit, recorded by a digitizer running at 20 KHz. Figure 5 shows a three-dimensional plot of x_n, y_n and z_n from the circuit, showing how the chaotic signal from the map fills the x-y-z volume in the phase space. Plots of x_n or y_n vs. z_n show the same space-filling property. To test the uniformity of these points we partitioned the volume containing the points into various numbers of bins, 64, 512, and 4096. For a uniform, randomly distributed set of points the number of points in each bin m would have a standard deviation of $\sqrt{m}$. We compared the standard deviations of the volume preserving maps and circuits from uniformity with the standard deviations found in typical chaotic attractors like the Lorenz [16] and the Lorenz84 [17].

The Lorenz84 is a particularly good comparison since its attractor is more space filling than most with a fractal dimension of around 2.4 whereas the original Lorenz has a fractal dimension of slightly over 2.0. The volume-preserving systems had deviations of 2 to 6 times those of the uniform distribution. The Lorenz attractors had deviations from

10 to 30 times those of the uniform distribution. This even though the volume preserving sets had fractal dimensions only slightly larger than the Lorenz84 system, namely 2.6.

Figure 6 is the power spectrum of the transmitted signal w_n from the circuit (defined in eq. (3)). The power spectrum does not roll off until about 0.6 times the clock frequency of 6 KHz. Figure 7 shows the autocorrelation for the signal w_n. The autocorrelation function drops to zero in 3 clock cycles. The output of the circuit changes only every 2 clock cycles, so the output signal w_n is almost delta function correlated. The output signal w_n closely resembles white noise.

Figure 8 shows the synchronization of the *x*' variable in the response circuit to the *x* variable in the drive circuit. Because of the transformation used in eq. (3) to produce $\tilde{z}$, the Lyapunov exponent for the *x*' subsystem in eq. (3) is $-\infty$. There are some points off the diagonal axis in Fig. 8, indicating that the response circuit occasionally became desynchronized from the drive. The largest source of error between the drive and response circuits was the discontinuous modulus function.

The Lyapunov exponent for the *y*' subsystem was ln(1/3), so the synchronization of the *y*' subsystem in the circuit was not as good as for the *x*' subsystem. The *y*' subsystem had more large departures from synchronization (caused by the mismatch of the modulus function) than the *x*' subsystem. Larger subsystem Lyapunov exponents cause the response system to take longer to recover from errors, so synchronization is worse.

IV. Other chaotic maps and signal mixing functions

Reproducing the modulus function in the chaotic map circuit described above is not easy because the modulus function is discontinuous. It is possible to replace the modulus function with a continuous sawtooth function which still "folds" the trajectories back into the original phase space area, but that is easier to reproduce in a circuit. We would like all of the dynamical variables to remain between some limits, such as ±1.0. When a dynamical variable *x* goes beyond 1.0, instead of shifting it (modulus, as above) we replace x with $2–x$. If x is less than -1.0, we replace x with $2+x$. We continue this folding until x is between ±1.0. When plotted against x this gives a "sawtooth" function much like the tent map. Sawtooth functions will give power spectra that are less broad than the spectra one obtains from modulus functions, so there is some trade-off in making a circuit that is more easily reproduced.

V. Conclusions

Simple chaotic circuits may produce "white noise" signals similar to those produced by conventional pseudonoise generators. The self-synchronizing nature of chaotic circuits makes synchronizing chaotic pseudonoise circuits far simpler than synchronizing conventional pseudonoise circuits. Chaotic map circuits using either modulus or sawtooth nonlinearities may be built, depending on how broad the signal spectrum must be and how reproducible the chaotic circuit must be. The low correlations and broad spectra of chaotic circuits might make them useful for generating large numbers of spreading codes for spread spectrum systems.

Manuscript received: ________________________________

T. L. Carroll and L. M. Pecora are with the U. S. Naval Research Lab, Code 6343,
4555 Overlook Ave. SW, Washington, DC 20375

References

[1] L. M. Pecora and T. L. Carroll, "Synchronization in Chaotic Systems," *Phys. Rev. Lett.*, vol. 64, pp. 821-824, Feb. 1990.

[2] L. M. Pecora and T. L. Carroll, "Driving Systems with Chaotic Signals," *Phys. Rev. A*, vol. 44, pp. 2374-2383, August 1991.

[3] K. M. Cuomo and A. V. Oppenheim, "Circuit Implementation of Synchronized Chaos with Applications to Communications," *Phys. Rev. Lett.*, vol. 71, pp. 65-68, July 1993.

[4] K. M. Cuomo, A. V. Oppenheim and S. H. Strogatz, "Synchronization of Lorenz-Based Chaotic Circuits with Applications to Communications," *IEEE Trans. CAS*, vol. 40, pp. 626-633, Oct. 1993.

[5] K. Murali and M. Lakshmanan, "Transmission of signals by synchronization in a chaotic Van der Pol-Duffing oscillator," *Phys. Rev. E*, vol. 48, pp. 1624-1626, Sept. 1993.

[6] U. Parlitz, L. O. Chua, L. Kocarev, K. S. Halle and A. Shang, "Transmission of Digital Signals by Chaotic Synchronization," *Int. J. Bifurc. and Chaos*, vol. 2, pp. 973-977, Sept. 1992.

[7] S. Hayes, C. Grebogi, E. Ott and A. Mark, "Experimental Control of Chaos for Communication," *Phys. Rev. Lett.*, vol. 73, pp. 1781-1784, Sept. 1994.

[8] J. F. Heagy and T. L. Carroll, "Chaotic Synchronization in Hamiltonian Systems," *Chaos*, vol. 4, pp. 385-390, 2 1994.

[9] R. C. Dixon, *Spread Spectrum Systems with Commercial Applications*. New York: Wiley, 1994.

[10] K. Godfrey, *Perturbation Signals for System Identification*. New York: Prentice-Hall, 1993.

[11] N. Gershenfeld and G. Grinstein, "Entrainment and Communication with Dissipative Pseudorandom Dynamics," *Phys. Rev. Lett.*, vol. 74, pp. 5024-5027, June 1995.

[12] L. M. Pecora and T. L. Carroll, "Synthesizing and Using Volume-Preserving, Synchronized Chaotic Systems," vol. in preperation, pp. 1996.

[13] A. J. Lichtenberg and M. A. Lieberman, *Regular and Stochastic Motion*. New York: Springer-Verlag, 1983.

[14] T. L. Carroll, J. F. Heagy and L. M. Pecora, "Transforming signals with chaotic synchronization," *Phys. Rev. E*, vol. 54, pp. 4676-4680, Nov. 1996.

[15] J. H. Peng, E. J. Ding, M. Ding and W. Yang, "Synchronizing Hyperchaos with a Scalar Transmitted Signal," *Phys. Rev. Lett.*, vol. 76, pp. 904-907, Feb 1996.

[16] E. N. Lorenz, "Deterministic non-periodic flow," *Journal of Atmospheric Science*, vol. 20, pp. 130-141, 1963.

[17] E. N. Lorenz, *Physica D*, vol. 13, pp. 90, 1984.

Figure captions.

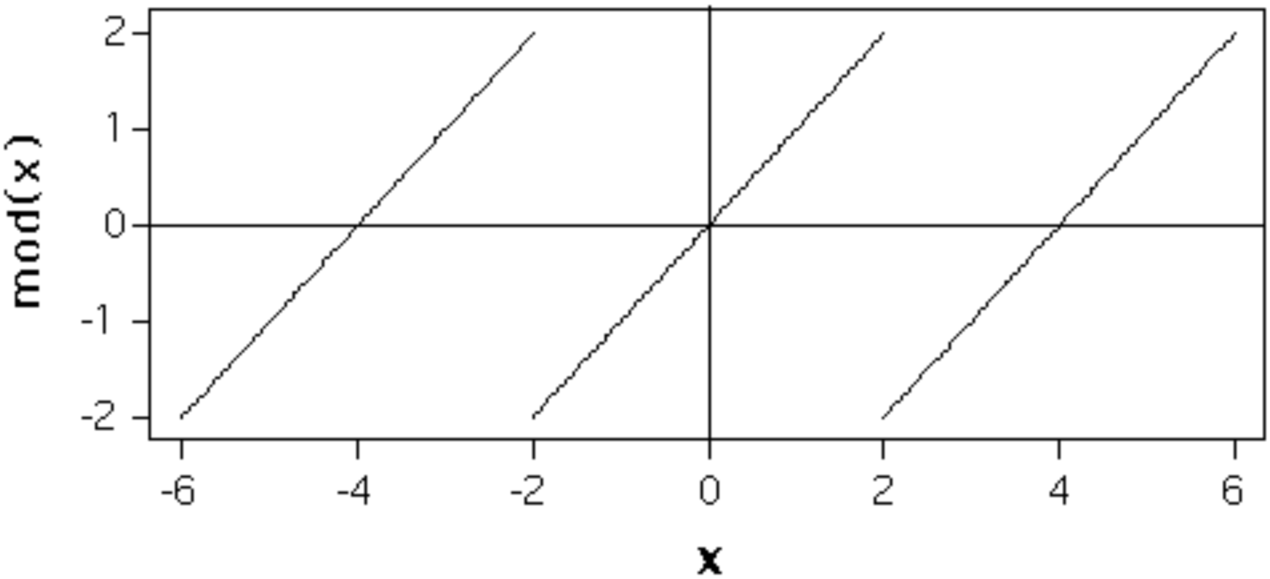

Fig. 1. Modulus function used for the map of eq. (1).

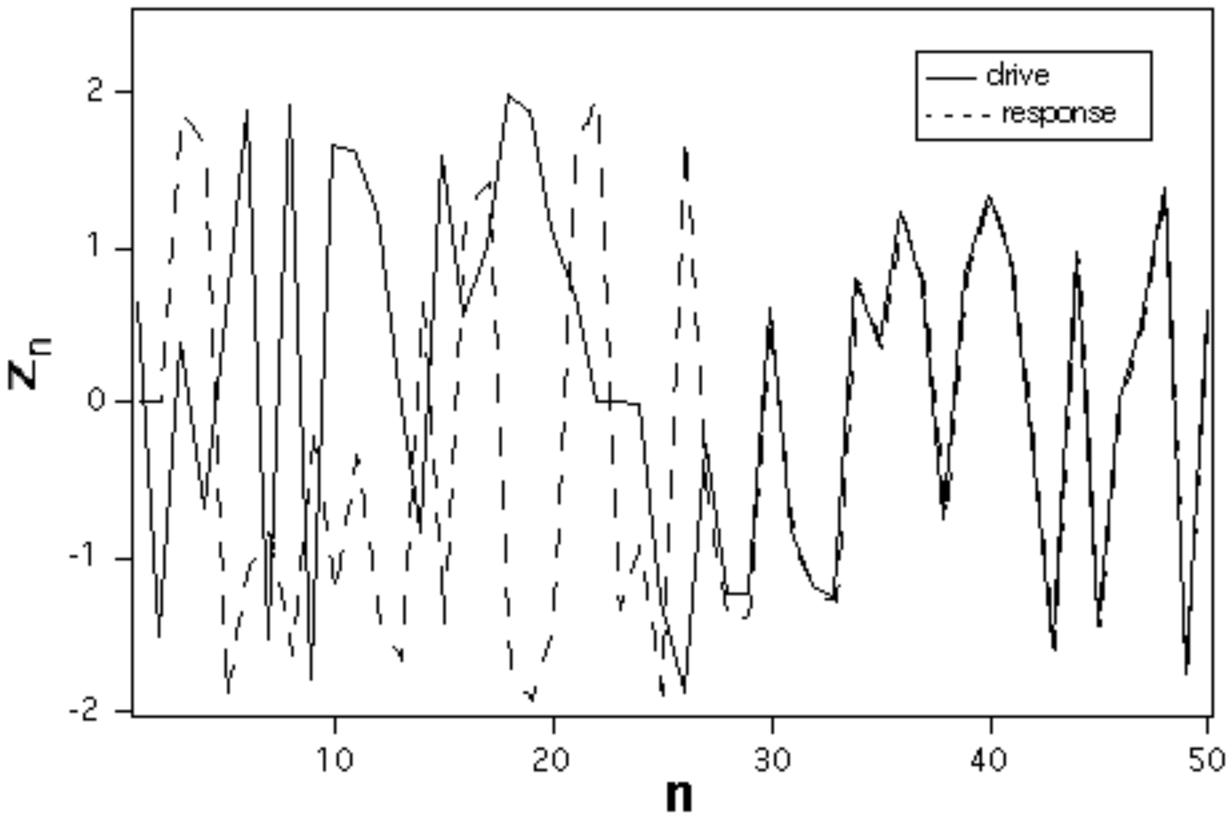

Fig. 2. The solid line shows *z* from the drive system and the dotted line shows *z*' from the response system of eqs (1) and (3) as the response system approaches synchronization.

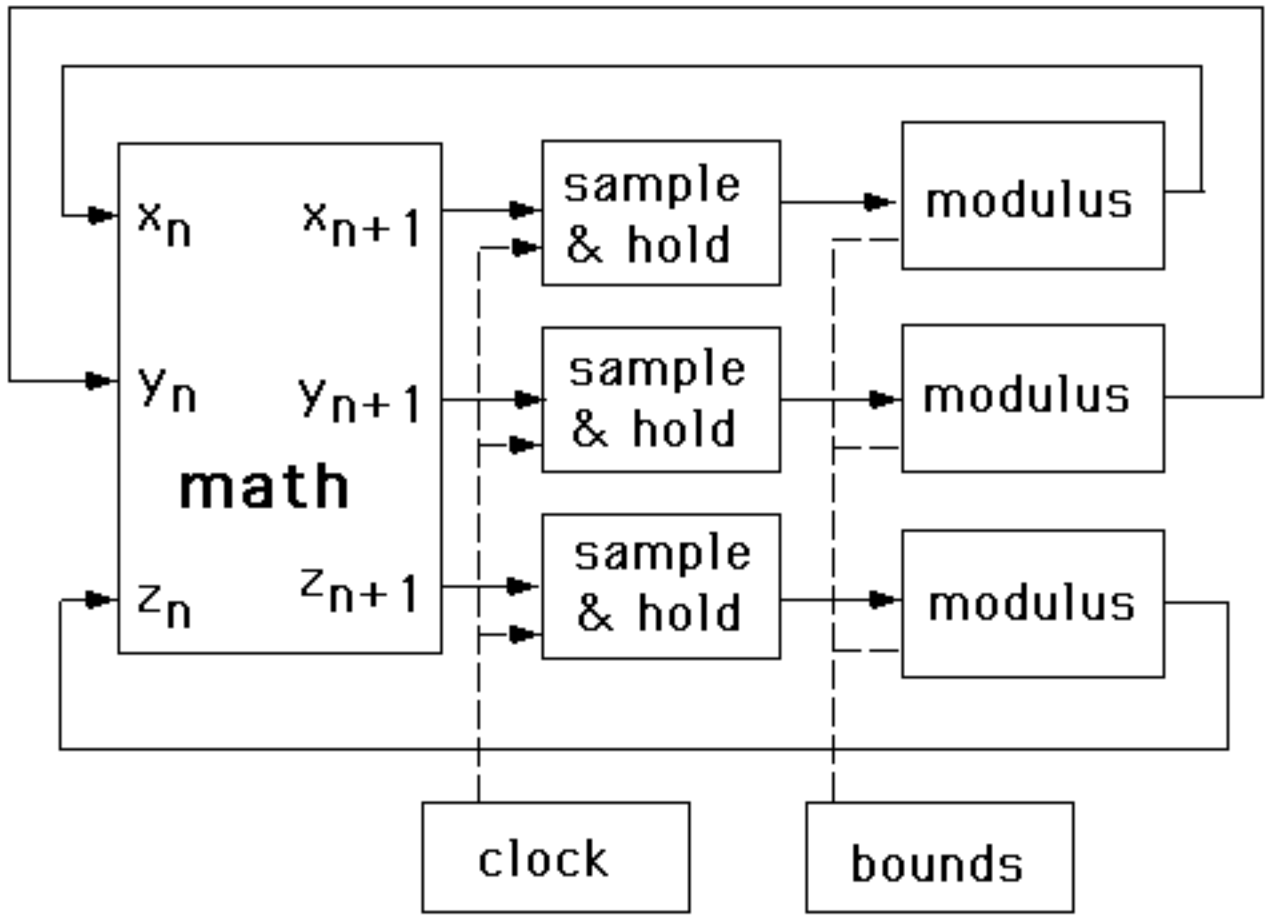

Fig. 3. Block diagram of the map circuit.

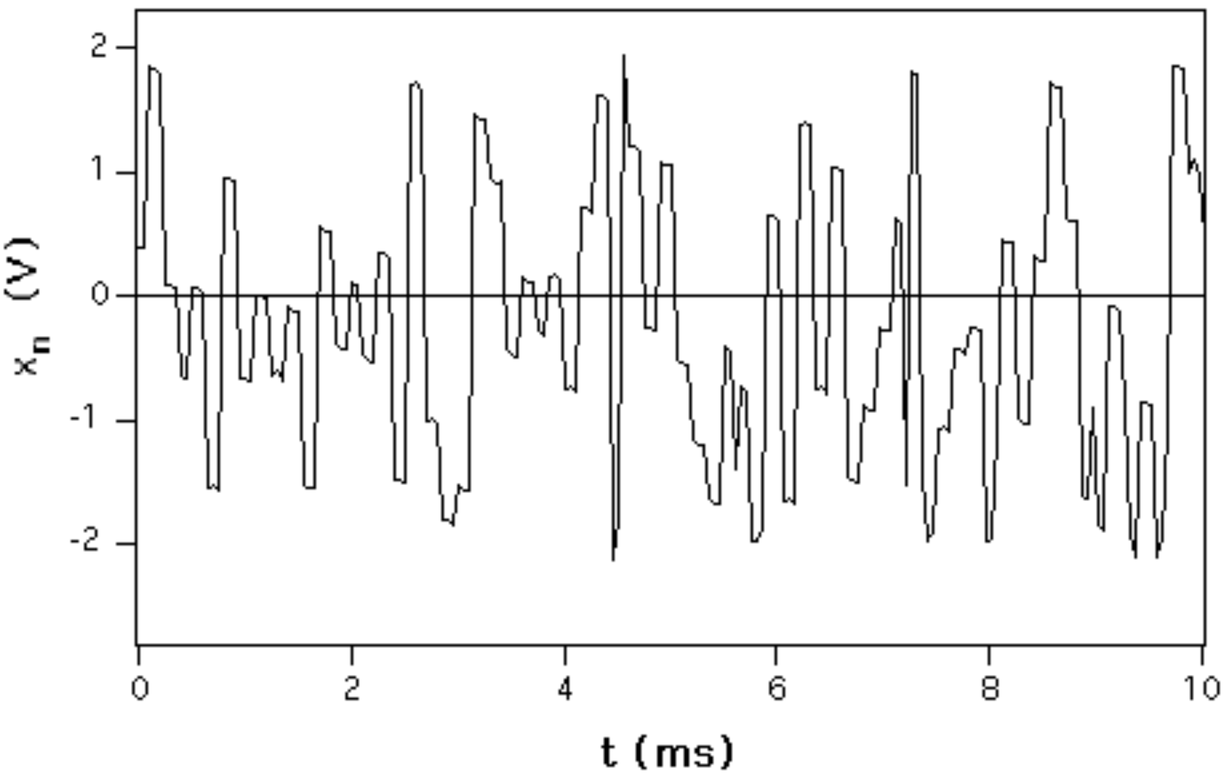

Fig. 4. Time series of the x_n signal from the map circuit, recorded by a digitizer at a rate of about 3 digitized points per output cycle.

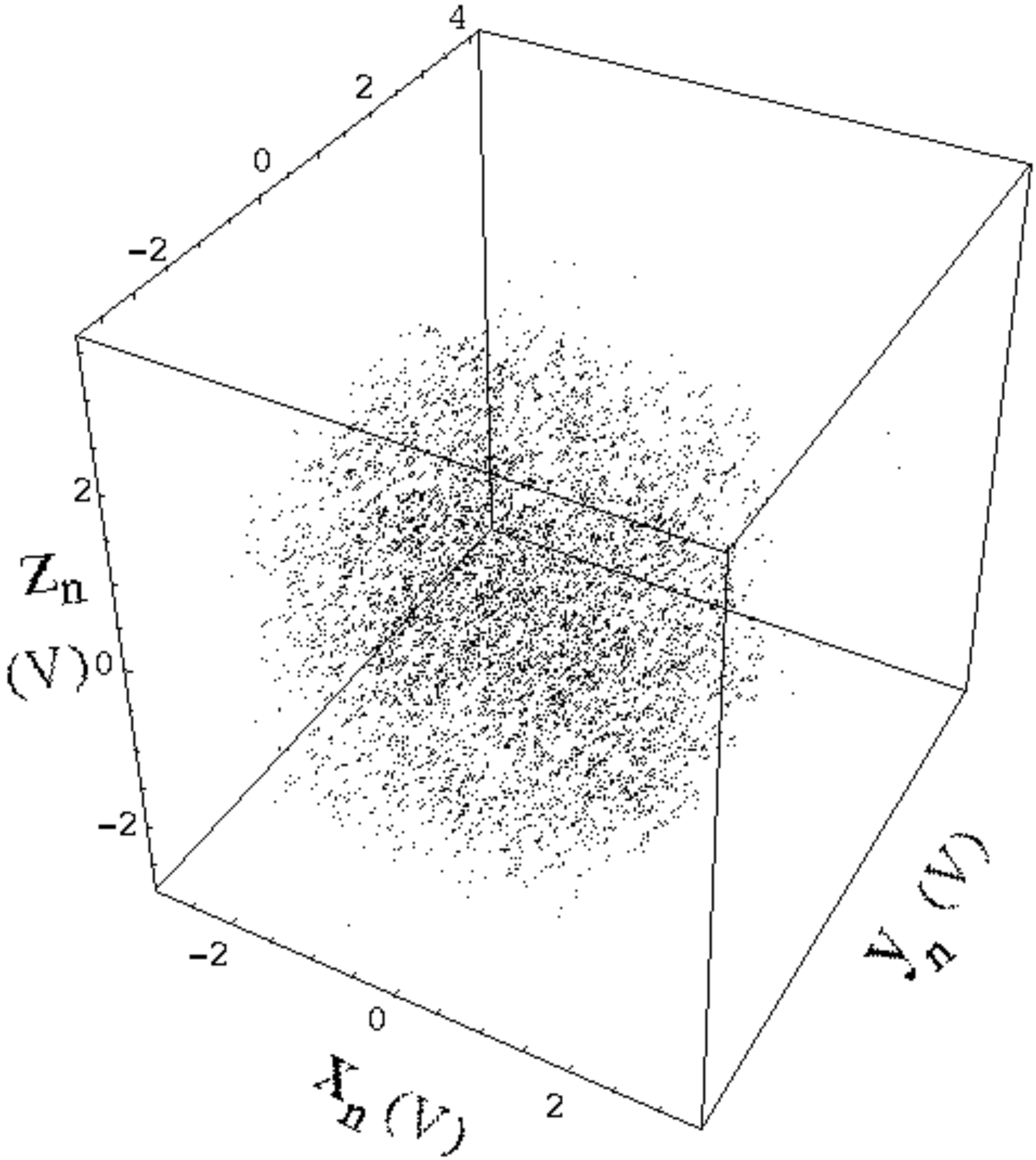

Fig 5. Plot of x_n, y_n and z_n signals from the circuit.

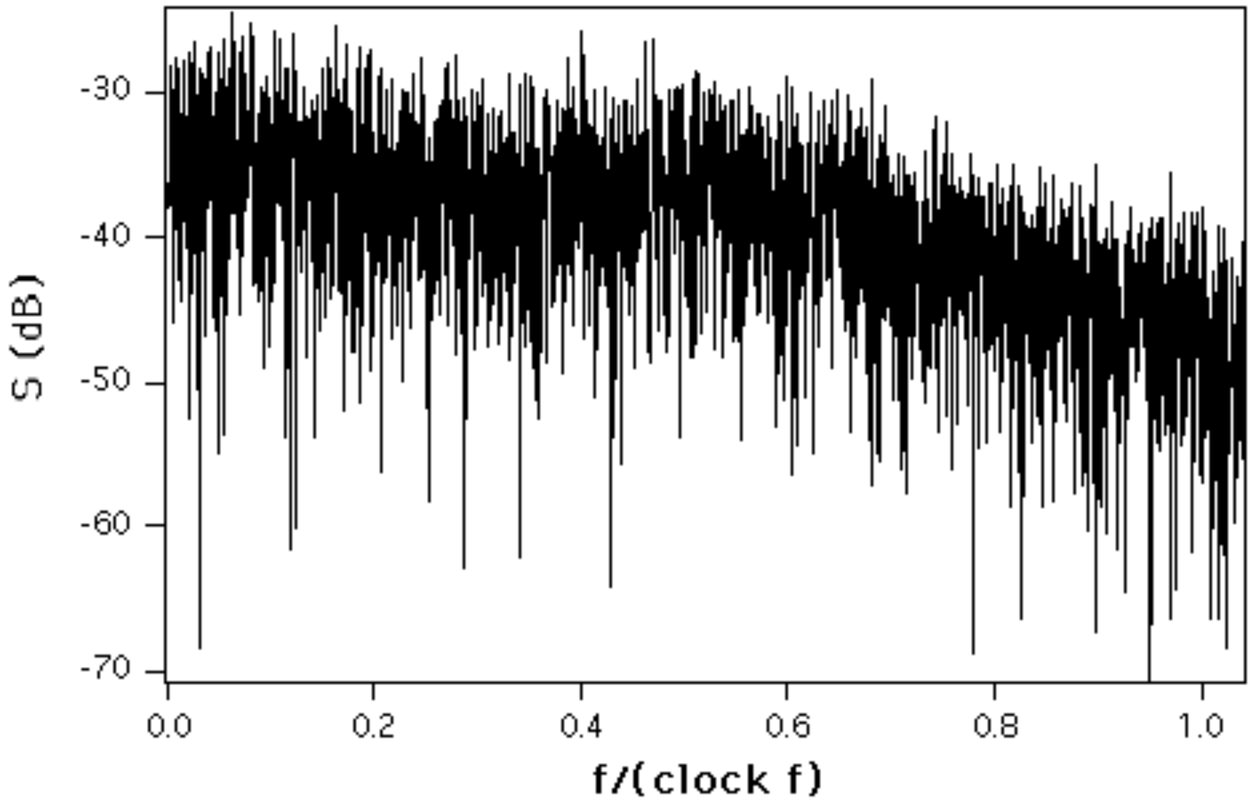

Fig. 6. Power spectrum S of the transmitted signal w_n (defined in eq. (3)) from the map circuit with a clock frequency of 6 kHz. The frequency is plotted as a fraction of the clock frequency.

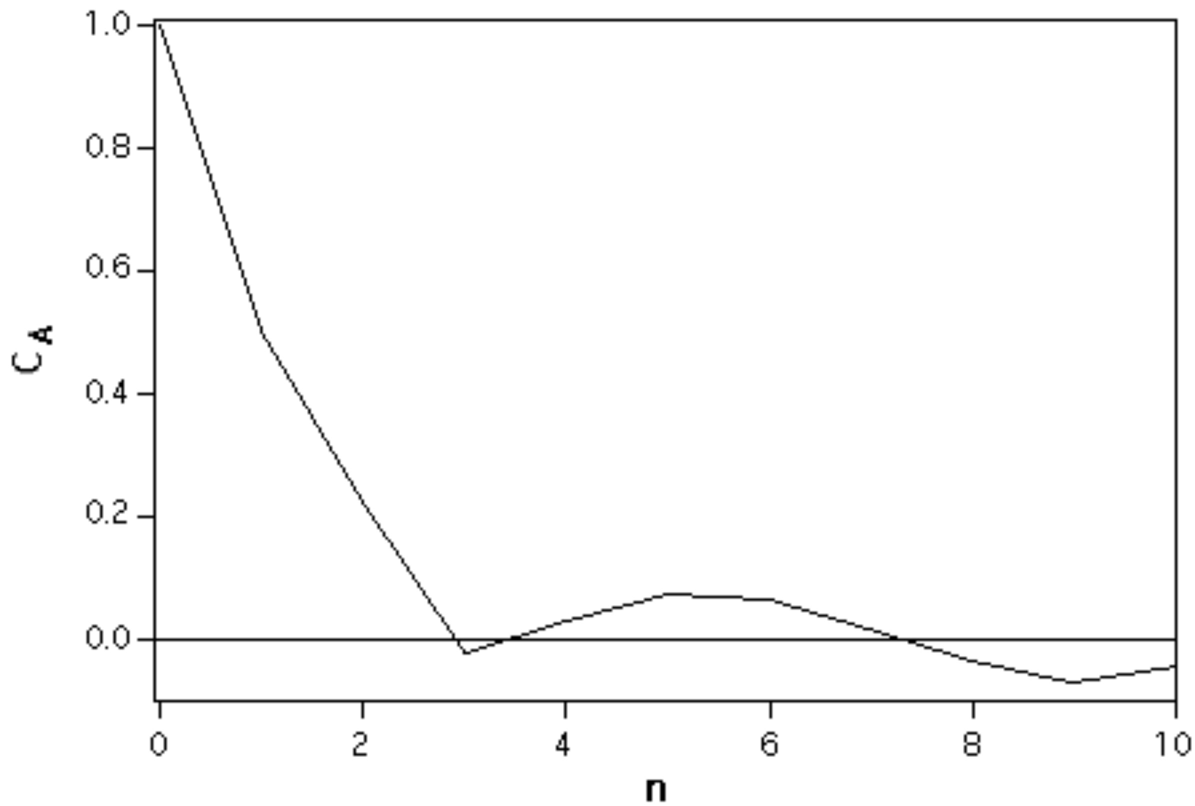

Figure 7. Autocorrelation function C_A for the w_n (defined in eq. (3)) signal from the map circuit as a function of the clock cycle n. The w_n signal changes every 2 clock cycles, so the autocorrelation function goes to zero before 2 output cycles have been completed.

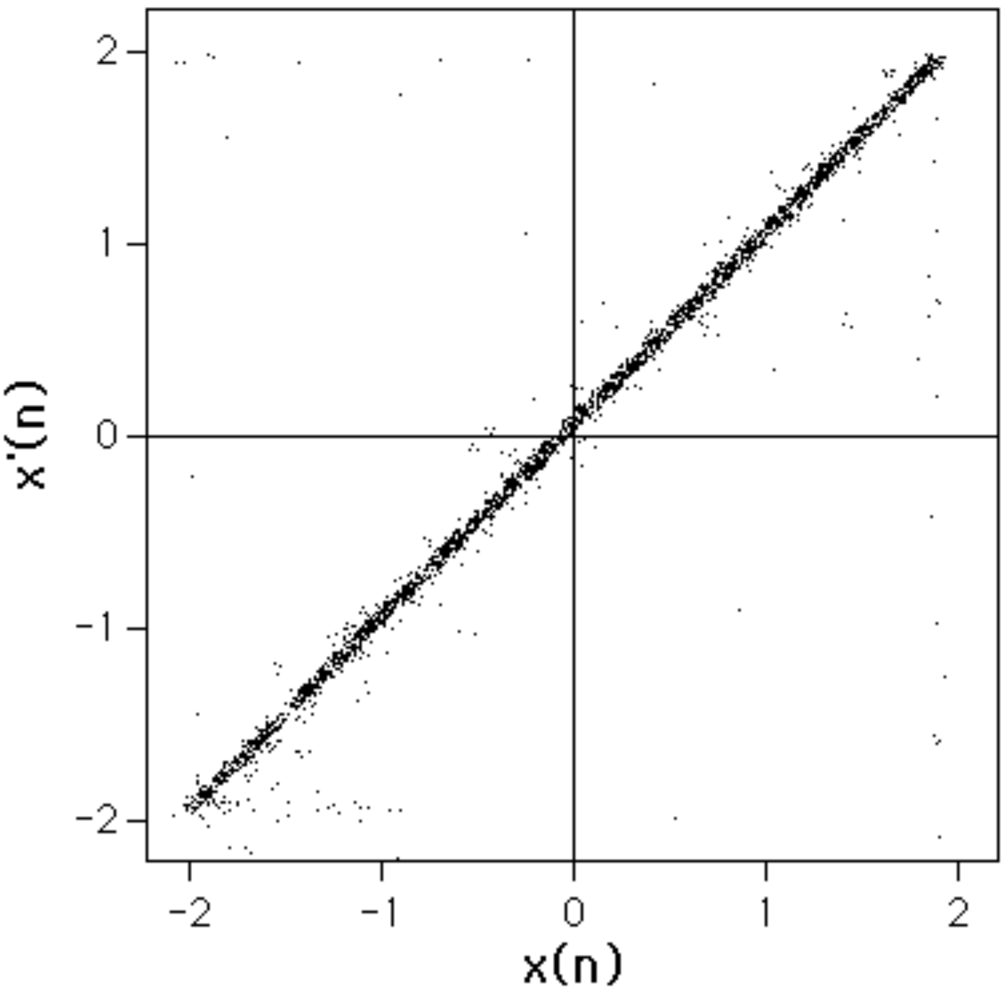

Figure 8. *x′* from the response circuit vs. *x* from the drive circuit showing that the response circuit does synchronize to the drive.